

Adsorptive performance of calcined *Cardita bicolor* for attenuating Hg(II) and As(III) from synthetic and real wastewaters

Abolfazl Teimouri*, Hossein Esmaeili**, Rauf Foroutan**, and Bahman Ramavandi***,†

*Department of Chemical Engineering, School of Chemical Engineering, Kherad Institute of Higher Education, Bushehr, Iran

**Department of Chemical Engineering, Bushehr Branch, Islamic Azad University, Bushehr, Iran

***Department of Environmental Health Engineering, Bushehr University of Medical Sciences, 7518759577 Bushehr, Iran

(Received 13 September 2017 • accepted 5 November 2017)

Abstract–The first application of calcined *Cardita bicolor* oyster shell (CCBS) for Hg(II) and As(III) adsorption from synthetic and real wastewaters was tested. The main elements in CCBS structure were carbon, oxygen, magnesium, phosphorus, and calcium. Effects of different parameters like initial pH, contact time, temperature, and CCBS dosage were assessed. The results showed that the maximum recovery of Hg(II) and As(III) adsorption was determined as $C_0=10$ mg/L, $t=80$ min, $T=25$ °C, CCBS dosage=5 g/L, and pH=6 (for mercury ion) and 7 (for arsenic ion). In these conditions, 95.72% Hg(II) and 96.88% As(III) were removed from aqueous solution. The correlation coefficient (R^2) values for both adsorbates were obtained >0.98 and >0.96 for Langmuir and Freundlich isotherm models, respectively. Pseudo-second-order kinetic model was more capable to describe kinetic behavior of adsorption process of both metal ions in comparison with pseudo-first-order model. The half life ($t_{1/2}$) value for Hg(II) and As(III) with initial concentration of 10 mg/L was 4.032 and 4.957 min, respectively. Moreover, thermodynamic parameters of enthalpy (ΔH°), entropy (ΔS°), and Gibbs free energy (ΔG°) were investigated. Two real wastewaters obtained from a leather factory and a landfill leachate were successfully treated using CCBS. The results confirmed that adsorption process of metals ions was exothermic and spontaneous.

Keywords: *Cardita bicolor*, Adsorption Isotherm, Hg(II), As(III), Kinetic Behavior, Real Wastewater

INTRODUCTION

Industrial wastewaters contain high amount of organic and inorganic toxic contaminants like heavy metals. These toxic metals are discharged into the water bodies and have serious effects on the quality of water bodies [1]. Toxic heavy metals are carcinogenic, and if the metals are not removed from wastewater, they can deteriorate the environmental quality and contaminate the food chain [2,3].

Among toxic and hazardous heavy metals, mercury can cause water and air pollution [4,5]. It is non-biodegradable and considerably toxic and can be released into the environment through different processes such as mining and metals purification, cement production plants and natural gas processing [6,7]. Allowable amount of mercury ion in the drinking water based on World Health Organization (WHO) recommendation is 0.001 mg/L [8]. Increasing the mercury ion in the human body can damage the cells and central nervous system and inhibit the activity of enzymes [2].

Arsenic ion is another toxic and hazardous metal in the environment. It is produced during natural process of slate and sediment washing and human activities including mining, burning fossil fuels, and the use of pesticides and insecticides and enters into the environment [9]. Arsenic can be transferred into human bodies or

other creatures through drinking water and/or food chain. It causes various diseases such as skin, lung, and kidney cancer and nervous disorders, weakening of muscles, anorexia and nausea [10]. Maximum allowable amount of As(III) in the drinking water was set as 10 μ g/L based on WHO, European Union (EU), and United States Environmental Protection Agency (US EPA) [11].

In recent years, various methods such as chemical precipitation, solvent extraction, membrane processes, filtration, reverse osmosis, oxidation, ion exchange, and adsorption have been applied to remove heavy metal ions from wastewater [12-15]. However, some of these methods are not widely used due to high cost and low feasibility in the industrial scale [16]. Recently, adsorption method was frequently used as it is economically feasible, versatile, efficient, simple, and bio-compatible [17,18]. Besides, the adsorbate (here, heavy metals) and adsorbent could be recycled if desired [19], which makes the adsorption process more cost-effective. In the adsorption method, the utilization of low- or no-cost agricultural and biological waste materials has been highly considered. *Aspergillus flavus* biomass [20], *Rhizopus oryzae* biomass [14], *Malva sylvestris* [2], and *Sargassum oligocystum* [21] are instances of low-cost materials applied for heavy metals removal.

Although horticultural and agricultural wastes have been widely used to produce adsorbents, marine resources (except algae whose research on their adsorption characteristics is going to be completed) such as bivalves, crayfish, shrimp, and oyster are rarely used to produce adsorbents. Literature review showed that the marine resources, especially oysters shell wastes, have suitable properties

†To whom correspondence should be addressed.

E-mail: ramavandi_b@yahoo.com, b.ramavandi@bpums.ac.ir
Copyright by The Korean Institute of Chemical Engineers.

like having active groups of $-NH_2$, $-CH$, PO_4^{-3} , and $-OH$, nontoxic and insoluble in water [22,23] which make it attractive for the adsorption process. The main aim of this study was to use the calcined *Cardita bicolor* oyster shell (CCBS) as a bio-adsorbent to remove heavy metal ions of Hg(II) and As(III) from aqueous solution. Some types of the oysters are consumed by humans as food. Thus, the wastes of the oysters could be easily found in the kitchen wastes with served oyster or the coast of many seas. Effects of different parameters such as initial pH, CCBS dosage, temperature, and contact time were examined on the removal efficiency and adsorption capacity of mercury and arsenic ions. In addition, kinetic behavior, isotherm modeling and thermodynamic characteristics of the adsorption process were investigated. The surface morphology, mapping, functional groups, and structural elements of the CCBS were also studied. To the best of the authors' knowledge, there is no published research regarding the contaminant removal by CCBS.

EXPERIMENTAL

1. Adsorbent Preparation and its Characterizations

The *Cardita bicolor* oyster shell was collected from the northern coast of the Persian Gulf, Bushehr, Iran and then rinsed by running tap water to remove dirt. Afterwards, it was oven-dried at 105°C for 24 h. To carry out the calcining process, the oyster shell was placed in an electric furnace at $1,000^\circ\text{C}$ for 5 h. At the end of the period, the shell pieces were placed at room temperature to cool. Then, calcined shells were powdered and sieved using sieve No. 25 (ASTM E11) and stored in a waterproof container at room temperature for later usage.

To investigate CCBS surface before and after Hg(II) and As(III) adsorption, the scanning electron microscopy (SEM), mapping, and energy-dispersive X-ray spectroscopy (EDX) tests were carried out using a TESCAN MIRA3-FEG instrument. To make images from the surface of the bio-adsorbent, it was covered with a thin layer of gold and then studied under SEM. Determination of functional groups and bio-adsorbent properties was carried out through FTIR (Broker Victor 22). IR analysis performed by KBr tablets (sample: $KBr \approx 1:50$) and infrared spectrum of bio-adsorbent was located at $400\text{--}4,000\text{ cm}^{-1}$ range. The resolution was 4 cm^{-1} and the scans were sixteen times repeated and averaged for each sample and background to get the spectrum.

The surface area of CCBS was analyzed by methylene blue (MB) method according to our previous study [24]. Briefly, different MB concentrations (1–40 mg/L) were provided for plotting the calibration curve. Then, 2 g/L CCBS was poured in the MB solution with concentration of 20 mg/L and agitated at 200 rpm for around 1 h. After that, the mixture was passed through the Whatman filter paper. The MB concentration in the filtrate was measured using a spectrophotometer at 600 nm wavelength. The CCBS surface area was obtained using Eq. (1):

$$S_{MB} = \frac{C_{opt} \times A_{MB} \times A_V}{MV_{MB}} \quad (1)$$

where: S_{MB} (m^2/g) is the surface area of the CCBS, C_{opt} (mg/mg) is the amount of MB molecules adsorbed by the bio-adsorbent, A_{MB}

is the area occupied by a molecule of MB, A , is Avogadro's number ($=6.02 \times 10^{23}$ molecules per mole), and MV_{MB} is the molecular weight of MB ($=319.87\text{ g/mol}$).

2. Solutions

Initial stock solution of As(III) and Hg(II) was prepared by dissolving 1.7339 g $NaAsO_2$ and 1.3536 g $HgCl_2$ in 1,000 mL double distilled water, respectively. Each solution with required initial concentration was arranged by diluting stock solution. Initial pH of the working solutions was set by 1 M HCl and NaOH. All chemical materials in this study were bought from Merck Company and double distilled water applied in all experiments.

3. Adsorption Tests

Adsorption tests of As(III) and Hg(II) in aqueous solutions using bio-adsorbent of CCBS were implemented in a batch mode using Erlenmeyer flasks containing 100 mL of arsenic and mercury solutions (separately). The effects of initial pH, temperature, contact time, initial adsorbate concentration, and CCBS dosage parameters on the adsorption efficiency of metal ions were examined. The effect of initial pH was studied at the range of 2–10 and pH was measured using a digital pH-meter (Metrohm 744). To optimize the solution pH, adsorption tests carried out at 25°C , 5 g/L CCBS dosage, 10 mg/L initial concentration of pollutants, 60 min contact time, and 200 rpm shaking rate. The temperature effect was studied in temperature range of $25\text{--}55^\circ\text{C}$ and at various time intervals (5–120 min), with initial pH of 7, bio-adsorbent dosage of 5 g/L, and shaking rate of 200 rpm. The effect of bio-adsorbent dosage on the adsorption efficiency and adsorption capacity was also investigated at 0.5–10 g/L of CCBS dosage and 10 mg/L initial concentration of metal ions, 80 min contact time, 200 rpm shaking rate, 25°C temperature, and initial pH of 7 and 6 for As(III) and Hg(II), respectively.

Each test was repeated three times and the highest efficiency selected as optimized value. Residual arsenic ion content in the solutions was measured with the atomic fluorescence analyzer (AF-610D2, Beijing Ruili Co., Ltd., Beijing, China). This device uses acetylene and air mixture as fuel. Determination of Hg(II) in the solution was done using a atomic absorption spectrometry-cold vapor (UNICAM, model 929, UK). In all tests, the removal percentage of metal ions and adsorption capacity (q_e , mg/g) were calculated using following equations:

$$\% \text{Removal} = \left(\frac{C_i - C_f}{C_i} \right) \times 100 \quad (2)$$

$$q_e = \left(\frac{C_e - C_o}{W} \right) \times V \quad (3)$$

where: C_i , C_e , and C_f (mg/L) are the concentration of arsenic and mercury cations at initial, equilibrium, and studied times intervals, respectively. V (L) is the volume of solution and M (g) is the dry weight of CCBS.

4. Real Wastewaters Treatment

Two real wastewaters were sampled from a leather factory and landfill leachate to test the applicability of the CCBS adsorbent in the field. The leather factory is located in Lorestan, Iran. The leather wastewater was collected from the equalization tank of the wastewater treatment plant of the factory. The wastewater sample of the

factory was shipped to the laboratory at 4 °C within 4 h. The landfill leachate was taken from a pond beside a domestic solid waste landfill, Bushehr, Iran. The leachate was transferred to the laboratory within 0.5 h and passed through the 0.42 μm Whatman filter to remove the suspended solids and then subjected to the adsorption test.

Triplicate tests were performed at the conditions of CCBS=5 g/L, contact time=60 min, temperature=298.15 °K, shaking rate=200

rpm, pH=as per original. All parameters in this section were analyzed according to Standard Methods for Examination of Water and Wastewater [25].

RESULTS AND DISCUSSION

1. CCBS Properties

The surface area of the CCBS was obtained as 17.40 m²/g by

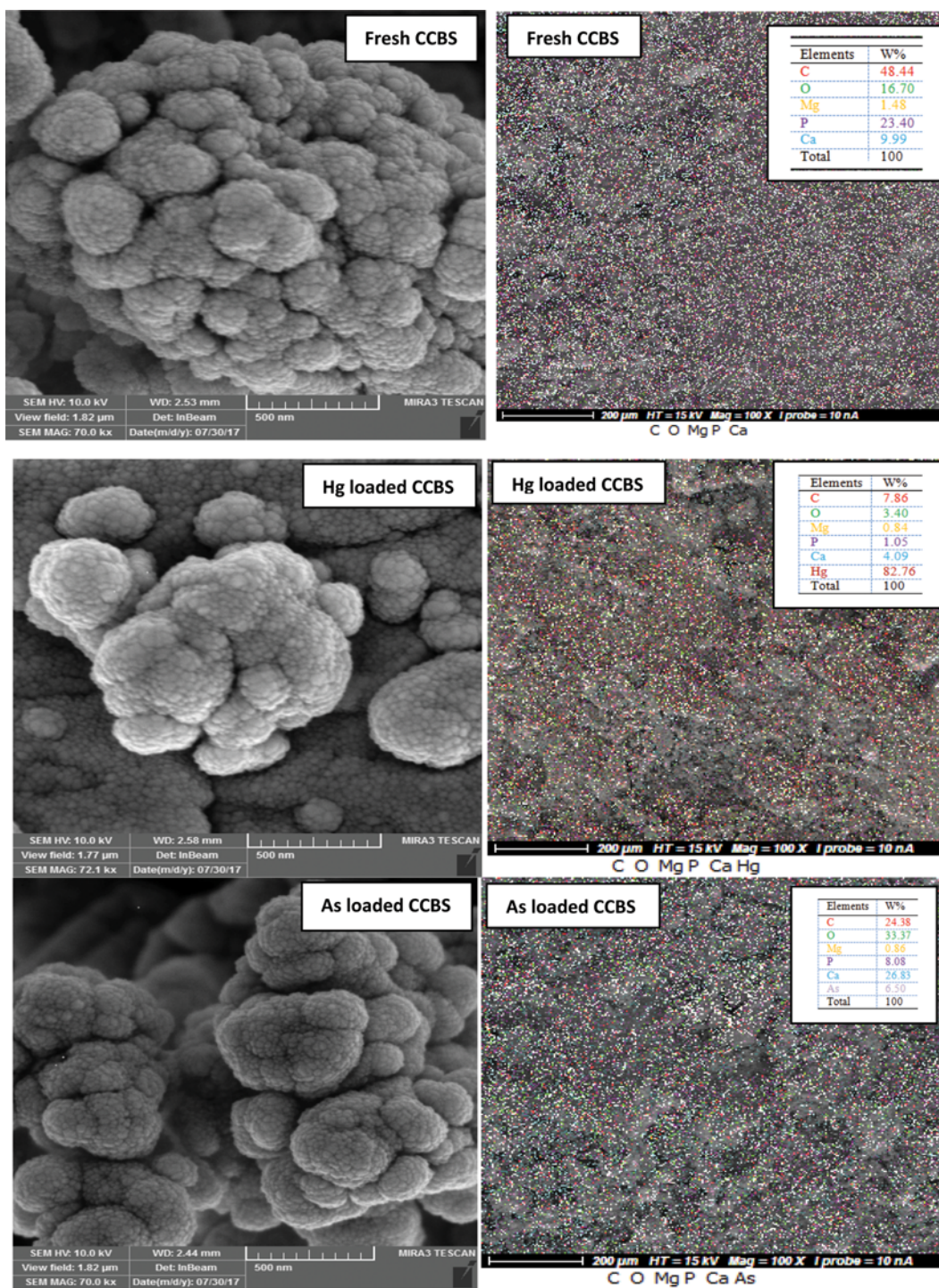


Fig. 1. SEM and mapping images and EDX results of fresh CCBS, Hg loaded CCBS and As loaded CCBS.

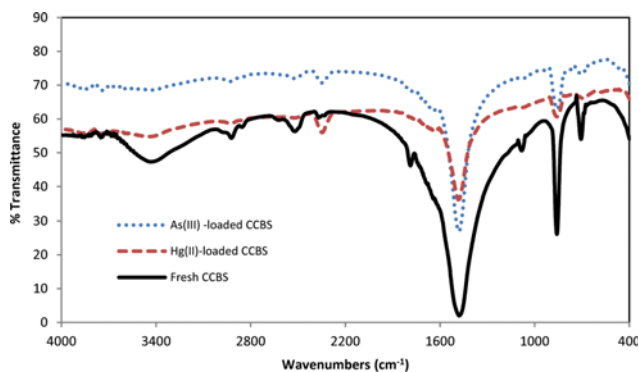


Fig. 2. FTIR spectra of fresh and Hg(II) and As(III) loaded CCBS.

the MB method. The surface area of the bio-adsorbent (using MB method) was within the range of those reported in other studies for calcined oyster shell (1.8 to 64.6 m²/g) by Brunauer-Emmett-Teller (BET) method [26]. The SEM images, elements, and distribution of elements for the CCBS adsorbent before and after adsorption process of Hg(II) and As(III) are depicted in Fig. 1. According to inset table in Fig. 1, the main elements in the CCBS structure are carbon, oxygen, magnesium, phosphor, and calcium. Fig. 1 also shows that the adsorbent surface has an ant's nest and crystalline form, with few holes on its surface. There is not much difference in the SEM images before and after adsorption process. However, the mapping and EDX analysis revealed that the CCBS adsorbent contain 82.7% Hg and 6.5% As after adsorption of Hg(II) and As(III). Therefore, it is deduced that the bio-adsorbent has eliminated mercury more effectively than arsenic from aqueous solution.

The infrared spectrum of fresh and used CCBS adsorbent is shown in Fig. 2. The fresh CCBS spectrum contained many peaks such as a broad peak at 3458.13 cm⁻¹, which can be due to vibrations of -OH functional group. There is also another minor peak at 2400-3,000 cm⁻¹ range, which can be dedicated to vibration and traction of -CH functional group. A peak at 1,477.22 cm⁻¹ range is owing to CO₃⁻² vibration in the structure of calcined *Cardita bicolor* oyster shell. Other peaks at 854.40 cm⁻¹ and 710.83 cm⁻¹ data range are related to PO₄⁻³ functional group. A notable point from the CCBS spectrum is that the nitrogen and sulfur groups are absent. Further, the adsorbent spectrum strongly changed after adsorption of arsenic and mercury ions, indicating the involvement of functional groups in adsorbing these ions.

2. Effects of pH

Previous researches showed that initial pH is a very important parameter in removal of heavy metal ions from aqueous solutions [27]. Adsorption tests of As(III) and Hg(II) from aqueous solution using CCBS were performed at pH 2-10, and the results are shown in Fig. 3. At initial pH=2, removal percentage of Hg(II) was very low (38.29%) and efficiency increased as pH changed from 2 to 6. Maximum Hg(II) removal of 94.67% occurred at pH=6. Based on Fig. 3, at acidic pH values (pH<6), the Hg(II) removal was low, that is due to competition between hydrogen cation (H⁺) and Hg(II) cation to relocate the active sites [28]. As pH approached to the neutral environment, the Hg(II) adsorption efficiency increased because cationic repulsive force between mercury ions and adsor-

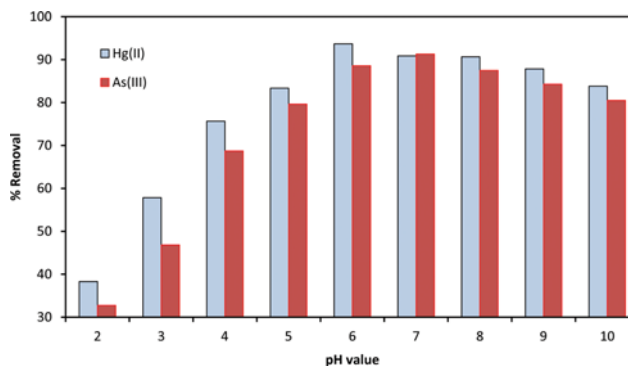


Fig. 3. Effects of solution pH.

bent surface and also competition effect with hydrogen cation decreased and removal percentage promoted. At pH values greater than 6 the adsorption efficiency of Hg(II) decreased, which may be caused by Hg(II) deposition [28]. Previous studies [2] revealed that increase the initial pH leads to increase in OH⁻ and competition of these groups with Hg(II) initiates and active sites are occupied with OH⁻ anions. Therefore, available active sites for Hg(II) adsorption decreased and resulted in the low percentage of Hg(II) adsorption [29]. Conclusively, pH=6 was determined as optimal pH for Hg(II) adsorption test using CCBS.

For As(III) adsorption tests, the initial pH of 7 was determined as the optimal pH (see Fig. 3). As pH changed from 2 to 7, the removal percentage of As(III) increased from 32.76% to 91.31%. But at alkaline pH values, the adsorption efficiency was decreased and reached 80.49% at pH 10. At initial pH of 2-7, arsenic has no ionic charge and converts to H₃AsO₃⁰, which cannot supply electrostatic force between metal ions and CCBS surface [30]. Previous studies showed that As(III) at pH=7 converts to H₃AsO₃, which can make a physical bond with neutral surface of the adsorbent [9]. At alkaline pHs (>7), As(III) converts to H₃AsO₃⁻ and the surface of the adsorbent also contains negative charges [31]. This situation occurs continuously on the surface of adsorbent and arsenic ion (converting to H₃AsO₃⁻ form) by increasing initial pH; therefore, a repulsion force is created between adsorbent surface and As(III) leading to reduction in the arsenic ion removal.

3. Effects of Temperature and Contact Time

Fig. 4 shows the effect of contact time on the adsorption effi-

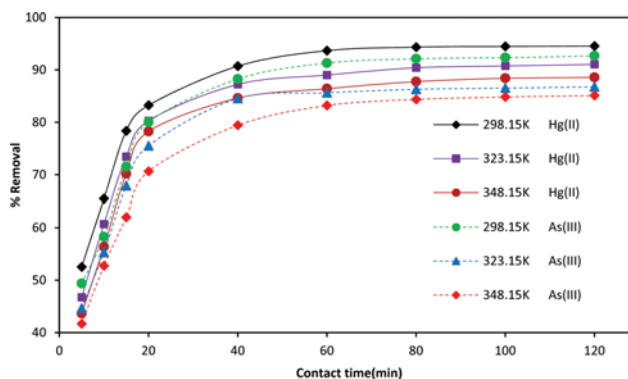


Fig. 4. Effects of temperature and contact time.

ciency of As(III) and Hg(II). According to Fig. 4, at initial contact times the removal rate of Hg(II) and As(III) by CCBS was high and more than 70% of the cations was removed after the contact time of 20 min. It is because at the beginning of the experiments, there were more active and unoccupied sites on the surface of the adsorbent. At contact time >80 min, there is no considerable change in mercury and arsenic ions removal. Therefore, the equilibrium time for the metal ions removal was determined as 80 min.

The initial solution temperature is known as a significant parameter in adsorption processes [32]. So, the effect of temperature on the adsorption of Hg(II) and As(III) from aqueous media was studied at conditions of 298.15-348.15 °K, 5 g/L CCBS dosage, and optimum pH. The results showed that at the t=80 min, by increasing the solution temperature from 298.15 °K to 348.15 °K the removal of Hg(II) and As(III) was reduced from 94.34% to 87.77% and 92.12% to 84.36%, respectively. Reduction in the removal recovery of Hg(II) and As(III) by increasing the solution temperature can be dedicated to a number of reasons like:

- 1) Increase in the tendency of metal ions to separate from the surface of CCBS and release into the solution phase.
- 2) Inactivating or destroying some of the active sites on the surface of adsorbent because of breaking the chemical bands.
- 3) Reduction in electrostatic force between metal ions and active sites on the surface of adsorbent at high temperatures.
- 4) Weakening the force between metal ions and active sites [33].

All these factors reduce the contact time between CCBS active sites and metal ions, resulting in the reduction of the adsorbates removal. Therefore, the solution temperature of 298.15 °K was selected as optimum temperature for the Hg(II) and As(III) removal using calcined *Cardita bicolor* oyster shell.

4. Effects of CCBS Dose

Adsorbent dosage is an important parameter in the adsorption process of heavy metal ions from aqueous solutions, because it determines the capability of adsorbent in contaminant removal process [34]. A study of CCBS dosage effect on As(III) and Hg(II) removal was performed and results are shown in Fig. 5. Increasing adsorbent dosage from 0.5 g/L to 10 g/L led to increasing the removal of Hg(II) and As(III) from 56.26% to 96.88% and 51.87% to 95.72%, respectively. This may be due to growth in the number of unsaturated active sites. The removal efficiency of Hg(II) and As(III) increased sharply to 5 g/L CCBS and afterwards remained

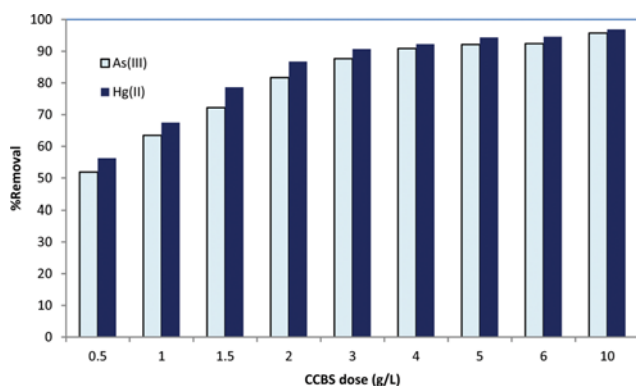


Fig. 5. Effects of CCBS dose.

constant with no considerable enhancement. It can be ascribed to integration and interaction of active sites or reduction in the concentration of metal ions in the aqueous solution to relocate the active sites. Therefore, the CCBS dose of 5 g/L was chosen as optimum dosage.

5. Isotherm Models

Adsorption isotherm models would be informative for full-scale designing of the studied adsorbent. There are different isotherm models to describe the behavior of isotherm processes. Two most common models are Freundlich and Langmuir models.

Langmuir model assumes that adsorption is performed through active sites on the surface of adsorbent. This model has been used successfully in many of homogeneous monolayer adsorption processes [35]. Linear form of Langmuir model can be presented as:

$$\frac{1}{q_e} = \frac{1}{K_L q_{max} C_e} + \frac{1}{q_{max}} \quad (4)$$

where: q_e is the amount of adsorbed metal ion in equilibrium state per gram of CCBS (mg/g), q_{max} and K_L are the constants of Langmuir model and as indications for adsorption capacity (mg/g) and adsorption energy (L/g), respectively. These constants are obtained by plotting $1/q_e$ versus $1/C_e$ as slope and intercept of linear Langmuir model, respectively. One of the other important parameter that defines the main characteristics of Langmuir model is R_L (separation factor or equilibrium parameter) that shows the state and condition of isotherm model. If $R_L > 1$, $R_L = 0$, $R_L = 1$, and $0 < R_L < 1$ then the process is defined to be undesirable, irreversible, linear, and desirable, respectively. The value of R_L is calculated using Eq. (5):

$$R_L = \frac{1}{1 + K_L C_e} \quad (5)$$

Freundlich isotherm model is an experimental model which can describe the adsorption of organic and inorganic compounds via various adsorbents. The linear form of this model is described as [20,36]:

$$\ln q_e = \ln K_f + 1/n \ln C_e \quad (6)$$

where: K_f and n are the model constants showing the relationship between adsorption capacity and adsorption intensity, respectively.

The linear regression plots and calculated parameters of Langmuir and Freundlich models are depicted in Fig. 6 and Table 1. According to Table 1, it was concluded that Langmuir model can slightly better describe adsorption behavior of Hg(II) and As(III) by CCBS than the Freundlich model. Correlation coefficient of Langmuir model for Hg(II) and As(III) adsorption was 0.9911 and 0.9862, respectively. Maximum value of the adsorption capacity for Hg(II) and As(III) was determined through Langmuir model as 42.01 mg/g and 60.97 mg/g, respectively. The q_{max} of the CCBS adsorbent is suitable in comparison with other adsorbents used for the Hg(II) or As(III) removal (see Table 2). R_L values were calculated 0.567 and 0.727 for Hg(II) and As(III), respectively, which proves that the adsorption of both metal ions by calcined *Cardita bicolor* oyster shell is appropriate and desirable.

The R^2 value of Freundlich model for Hg(II) and As(III) was also high and obtained to be 0.9797 and 0.9693, respectively. How-

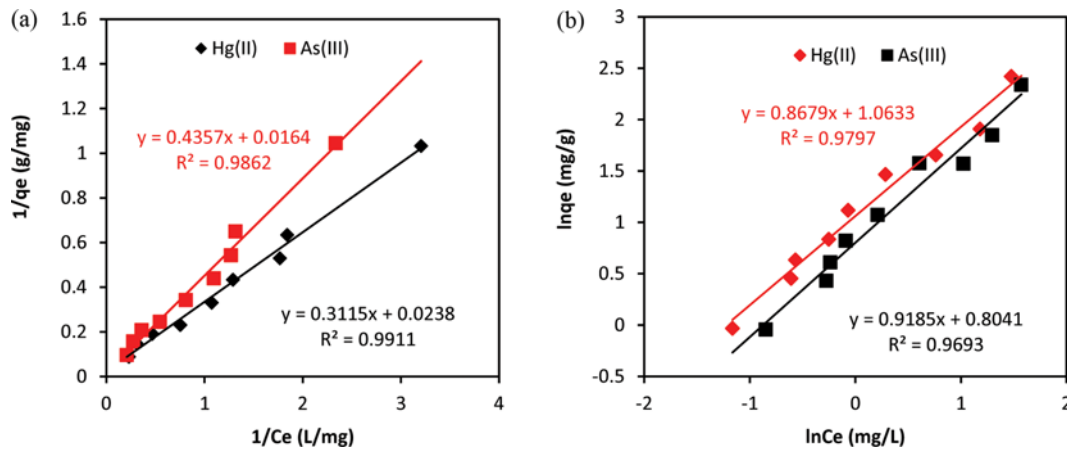


Fig. 6. Langmuir (a) and Freundlich (b) isotherm models for adsorption of Hg(II) and As(III) using CCBS.

Table 1. Results of isotherm modeling

Models	Parameters	Hg(II)	As(III)
Langmuir	q_m (mg/g)	42.02	60.98
	K_L (L/mg)	0.076	0.037
	R^2	0.9911	0.9862
	R_L	0.567	0.727
Freundlich	n	1.152	1.088
	K_f (mg/g (L/mg) ^{1/n})	2.895	2.234
	R^2	0.9797	0.9693

ever, in comparison with those for the Langmuir model, the Freundlich model is not appropriate for describing the adsorption behavior of mercury and arsenic cations by CCBS. It also showed that homogeneous sites compared with heterogeneous sites play more effective roles in mercury and arsenic adsorption. The value of parameter 'n' was calculated as 1.152 and 1.088 for Hg(II) and As(III), respectively. These values demonstrate that the adsorption of the pollutants onto the CCBS is a physical process [46].

6. Kinetic Studies

Kinetic studies of adsorption processes show the interactions

between metal ions in aqueous solution and the adsorbent. In the present study, kinetics of adsorption process performed at $C_0=10$ mg/L, pH=7 for arsenic, pH=6 for mercury, bio-adsorbent dosage=5 g/L, and temperature=298.15-348.15 °K. The well-known models of pseudo-first-order and pseudo-second-order were applied for description the Hg(II) and As(III) adsorption to CCBS.

Pseudo-first order kinetic model is defined as:

$$\ln(q_e - q_t) = \ln q_e - k_1 t \quad (7)$$

where: q_t (mg/g) is adsorbed ion per each gram of adsorbent at each time and k_1 is adsorption constant (1/min). Calculation of the adsorption constant (k_1) is done through plotting $\ln(q_e - q_t)$ versus t [12,47].

Pseudo-second-order kinetics model is described with the following equation:

$$\frac{1}{q_t} = \frac{1}{k_2 q_e^2} + \frac{t}{q_e} \quad (8)$$

where: k_2 is second-order kinetics rate constant (g/mg g) [48,49].

Linear graphs of pseudo-first and pseudo-second order models for mercury and arsenic adsorption using CCBS are shown in Fig. 7 and 8, respectively. The results of pseudo-first and pseudo-second

Table 2. Comparison of q_{max} (mg/g) of various adsorbents for Hg(II) and As(III) adsorption

Adsorbent	Hg(II)	As(III)	Reference
Biomass of <i>Spirogyra</i> species	156.7	-	[5]
Coal fly ash	0.44	-	[37]
Activated carbon impregnated with humic acid	17.12-22.32	-	[38]
Polyethylenimine modified-activated carbon	16.39	-	[39]
<i>Aspergillus Niger</i>	40.5	-	[40]
<i>Chlamydomonas reinhardtii</i> (Ca-alginate)	38.9	-	[41]
Tire rubber activated carbon-alumina composites	-	14.28	[42]
Tire rubber alumina composite	-	13.51	[42]
Zirconium oxide on alginate beads	-	32.3	[43]
Coconut (<i>Cocos nucifera</i> L.) fiber	-	0.1006	[44]
Cu-chitosan/Al ₂ O ₃	-	18.32	[45]
CCBS	42.02	60.98	This work

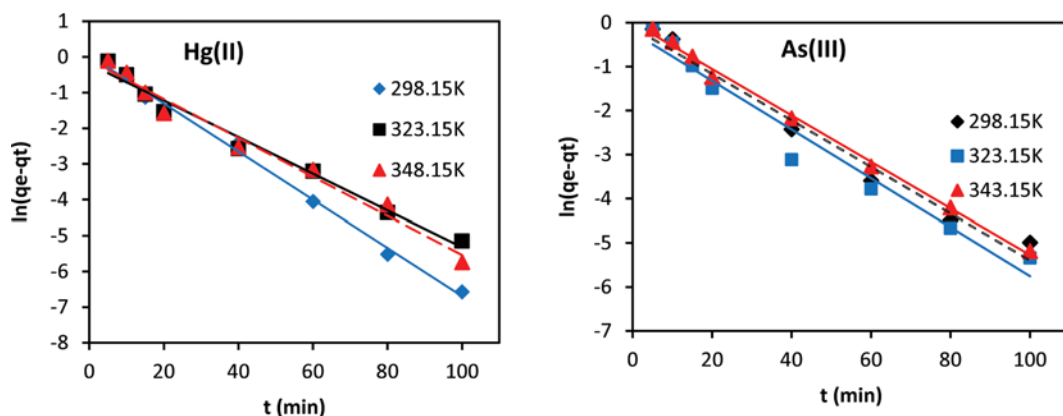


Fig. 7. Pseudo first order model.

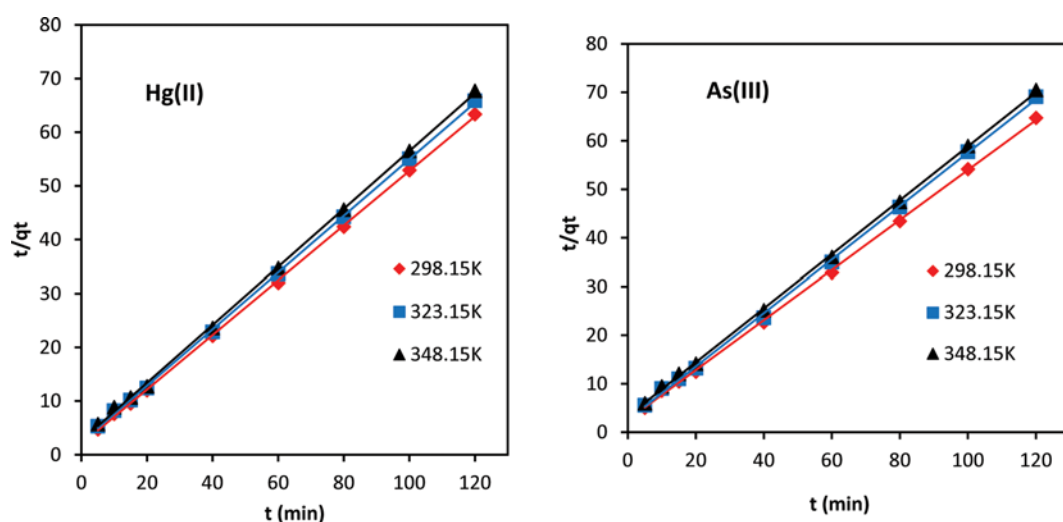


Fig. 8. Pseudo second order model.

Table 3. Results of adsorption kinetic study

Temperature (°K)	$q_{e,exp}$ (mg/g)	Pseudo-first-order			Pseudo-second-order		
		k_1 (1/min)	$q_{e1,cal}$ (mg/g)	R_1^2	k_2 (g/mg min)	$q_{e2,cal}$ (mg/g)	R_2^2
Hg(II)							
298.15	1.890	0.0674	1.042	0.9953	0.1265	1.968	0.9998
323.15	1.821	0.0513	0.823	0.9827	0.1175	1.899	0.9997
348.15	1.771	0.0545	0.915	0.9803	0.1096	1.856	0.9995
As(III)							
298.15	1.853	0.0529	0.898	0.9802	0.1038	1.944	0.9995
323.15	1.735	0.0553	0.804	0.9665	0.1161	1.819	0.9994
348.15	1.702	0.0527	0.998	0.9966	0.093	1.800	0.9997

ond order models are also summarized in Table 3.

According to the results, data obtained in the batch experiments follows pseudo-second order kinetic model because the values of $R_2^2 > R_1^2$ and $q_{e2,cal}$ parameter are more close to equivalent $q_{e,exp}$ values rather than $q_{e1,cal}$. This confirms higher ability of pseudo-second-order model to describe kinetic behavior of Hg(II) and As(III) adsorption using CCBS.

7. Kinetic Performance of CCBS

The performance of Hg(II) and As(III) adsorption by CCBS from synthetic wastewater was also evaluated based on the $q_{e2,cal}$ and k_2 parameters which obtained for pseudo-second-order model at 298.15 °K (see Table 3) and Eqs. (9)-(12) [50]:

$$R_t = k_2 q_{e2,cal} \tag{9}$$

$$F_{ae} = \frac{1}{1 + k_2 t_w q_{e2.cal}} \quad (10)$$

$$t_{1/2} = \frac{1}{k_2 q_{e2.cal}} \quad (11)$$

$$t_x = \frac{S}{k_2 q_{e2.cal}} \quad (12)$$

where: R_i (min^{-1}) denotes the second-order rate index, F_{ae} (dimensionless) denotes the approaching equilibrium factor, t_w (min) denotes the longest contact time, $t_{1/2}$ (min) denotes the required contact time for reaching the initial Hg(II) and As(III) concentration to the half level by the adsorbent, t_x (min) is the required contact times for the determined value of fractional adsorption ($X = q_t / q_{e2.cal}$) and S denotes equal to ' $X/(1-X)$ '. If the value of F_{ae} within the range of 0.1-1, 0.1-0.01, and <0.01 , then the kinetic is evaluated as slightly approaching equilibrium, well approaching equilibrium, and drastically approaching equilibrium, respectively. The value of F_{ae} was 0.0325 and 0.0396 for Hg(II) and As(III), and it was determined that the adsorption process well reached equilibrium. The value of R_i and $t_{1/2}$ factors was obtained to be 0.248 min^{-1} and 4.032 min for Hg(II) and 0.2017 min^{-1} and 4.957 min for As(III), respectively. The small value of half-life for both adsorbates showed that the rapid adsorption process occurred using CCBS. R_i is a key parameter affecting the value of fractional adsorption. Thus, it was applied to calculate the data of t_x for various X values of Hg(II) and As(III) adsorption by the CCBS adsorbent and the results are in Table 4. Results of CCBS kinetic performance would be informative for designing of Hg(II) and As(III) adsorption.

8. Thermodynamic Study

Thermodynamic parameters like free Gibbs energy (ΔG°), enthalpy (ΔH°), and entropy (ΔS°) were studied at temperature ranges

Table 4. Required operating times for various fractional adsorption values

Heavy metals	Operating time, t_x	Fractional adsorption, X	t_x Value (min)
Hg(II)	$t_{0.528}$	0.528	4.508
	$t_{0.692}$	0.692	9.056
	$t_{0.828}$	0.828	19.411
	$t_{0.8805}$	0.8805	29.709
	$t_{0.959}$	0.959	94.314
	$t_{0.9907}$	0.9907	429.54
	$t_{0.9978}$	0.9978	1828.81
	$t_{0.9992}$	0.9992	5036.29
As(III)	$t_{0.532}$	0.532	5.632
	$t_{0.628}$	0.628	8.368
	$t_{0.771}$	0.771	16.688
	$t_{0.863}$	0.863	31.229
	$t_{0.952}$	0.952	98.329
	$t_{0.985}$	0.985	325.562
	$t_{0.9939}$	0.9939	807.803
	$t_{0.9963}$	0.9963	1335.002

of 298.15-348.15 °K. These parameters estimate the type of process in terms of exothermic or endothermic and feasibility of the process. ΔG° is defined as follows [17]:

$$\Delta G^\circ = -RT \ln K_D \quad (13)$$

where R is the universal gas constant (8.314 J/mole °K) and T is absolute temperature in Kelvin. ΔH° and ΔS° are also defined with the following equations [51]:

$$\ln K_D = \frac{\Delta S^\circ}{R} + \frac{\Delta H^\circ}{RT} \quad (14)$$

$$K_D = \frac{C_{ad}}{C_e} \quad (15)$$

where C_{ad} and C_e are the amount of metal ions adsorbed onto the adsorbent surface and metal ion content of the solution phase, respectively. According to Eq. (14), the values of enthalpy and entropy are calculated by plotting $\ln K_D$ versus $1/T$ and consequently the slope and intercept of the graph determine the enthalpy and entropy, respectively.

Thermodynamic parameters were determined for adsorption process of mercury and arsenic ions, and the results are shown in Table 5. The ΔG° parameter of arsenic and mercury ion adsorption was obtained negative, showing the adsorption of Hg(II) and As(III) using CCBS was spontaneous. The enthalpy of adsorption process was attained -14.64 KJ/mol and -13.52 KJ/mol for mercury and arsenic ions, respectively, indicating that the process is exothermic for both adsorbates. Negative values for entropy implied that the collision of solid and liquid phases is reduced during the adsorption process [15].

9. Treatment of Real Wastewater Samples

As the final part of this work and to the field applicability of CCBS, two real wastewaters were examined. The results are depicted in Table 6. As specified in this table, sample 1 contained low level of organic materials (in the terms of BOD₅ and COD) and high levels of heavy metals. Both organic and inorganic materials decreased after treatment by CCBS. The As(III) content of the first sample was removed 60.49%.

In contrast, sample 2 (the landfill leachate) contained very low level of heavy metals and high amount of organic matter. All tested heavy metals were completely decreased using CCBS. However, the BOD₅ and COD parameters were slightly lowered.

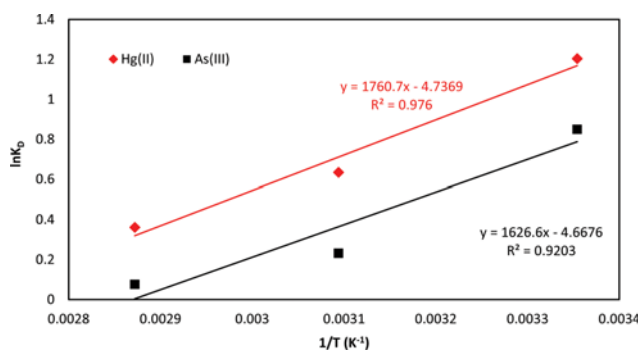
A point implied from treatment of two samples by CCBS is tending the final pH to the neutral (i.e., pH=7), which confirms the amphoteric property of the bio-adsorbent. This characteristic

Table 5. Adsorption thermodynamic parameters

Metal ions	T (°K)	ΔG° (KJ/mol)	ΔH° (KJ/mol)	ΔS° (J/mol °K)
Hg(II)	298.15	-2.98		
	323.15	-1.70	-14.64	-39.38
	348.15	-1.04		
As(III)	298.15	-2.11		
	323.15	-0.62	-13.52	-38.81
	348.15	-0.22		

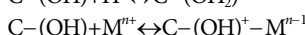
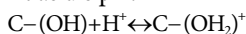
Table 6. Characteristics of real wastewater samples

Characteristics	Unit	Sample 1: Leather factory		Sample 2: Landfill leachate	
		Fresh	Treated	Fresh	Treated
As(III)	mg/L	10.25±0.12	4.05±0.11	0.136±0.04	No-detectable
Hg(II)	mg/L	No-detectable	No-detectable	0.98±0.08	No-detectable
As(V)	mg/L	7.42±0.13	2.5±0.09	0.83±0.07	No-detectable
Cr(VI)	mg/L	9.15±0.09	3.2±0.12	1.12±0.03	No-detectable
BOD5	mg/L	148.25±5.2	130.5±3.5	2110±43	2097±16
COD	mg/L	305.28±7.6	274.6±3.4	40789±25	4071±19
pH	-	6.250±0.15	07.1±0.04	7.97±0.2	7.22±0.14

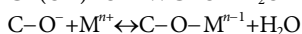
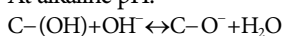
**Fig. 9. Linear relationship of $\ln K_D$ versus $1/T$ for thermodynamic parameters determination.**

can be justified by the fact that at acidic or alkaline conditions both adsorbate (mercury and arsenic ions) and H^+ or OH^- are simultaneously adsorbed onto CCBS but at different capacities. The binding of adsorbates, H^+ and OH^- on the adsorbent surface can be described as follows:

At acidic pH:



At alkaline pH:



CONCLUSIONS

The calcined *Cardita bicolor* oyster shell (CCBS) was tested for Hg(II) and As(III) removal from aqueous solution for the first time. The study was conducted in batch mode and the effects of different parameters including initial pH, temperature, contact time, and CCBS dosage were investigated. According to results, initial pH was the most effective parameter in the mercury and arsenic adsorption process in comparison with other studied parameters. The removal of Hg(II) and As(III) improved by increasing temperature, contact time, adsorbent dosage, and initial pH. The kinetic study revealed that adsorption process of mercury and arsenic ions using CCBS followed pseudo-second-order model. The q_{max} for Langmuir isotherm was determined to be 42.02 mg/g and 60.97 mg/g for Hg(II) and As(III), respectively. Thermodynamic

parameters like enthalpy, entropy, and Gibbs free energy were also examined, and results confirmed that the adsorption process of Hg(II) and As(III) with CCBS is exothermic and spontaneous. The performance of Hg(II) and As(III) adsorption by CCBS from synthetic wastewater was also evaluated based on approaching equilibrium factor, $t_{1/2}$, and fractional adsorption. Generally, the CCBS adsorbent for eliminating of Hg(II) and As(III) from synthetic and real wastewaters is cheap, facile, and efficient.

ACKNOWLEDGEMENTS

The authors are grateful to the Islamic Azad University, Bushehr Branch, Iran for providing technical support to carry out this work. The managers of Lorestan Leather Factory, Iran and Waste Management Organization, Bushehr, Iran are also acknowledged for allowing us to take wastewater and leachate samples. Thanks to the University of Tabriz, Iran for collaborations to perform the adsorbent characteristics.

REFERENCES

1. T. Robinson, *Waste Manag.*, **63**, 299 (2017).
2. B. Ramavandi, A. Rahbar and S. Sahebi, *Desal. Water Treat.*, **57**, 23814 (2016).
3. F. Saberzadeh Sarvestani, H. Esmaeili and B. Ramavandi, *3 Bio-tech*, **6**, 251 (2016).
4. A. Rezaee, B. Ramavandi and F. Ganati, *Pak. J. Biolog. Sci.*, **9**, 777 (2006).
5. A. Rezaee, B. Ramavandi, F. Ganati, M. Ansari and A. Solimani, *J. Biolog. Sci.*, **6**, 695 (2006).
6. K. Johari, N. Saman, S. T. Song, C. S. Chin, H. Kong and H. Mat, *Int. Biodeter. Biodegr.*, **109**, 45 (2016).
7. M. Leili, S. Farjadfar, G. A. Sorial and B. Ramavandi, *J. Environ. Manage.*, **204**, 531 (2017).
8. S.-T. Song, Y.-F. Hau, N. Saman, K. Johari, S.-C. Cheu, H. Kong and H. Mat, *J. Environ. Chem. Eng.*, **4**, 1685 (2016).
9. M. Aryal, M. Ziagova and M. Liakopoulou-Kyriakides, *Chem. Eng. J.*, **162**, 178 (2010).
10. M. Sánchez-Cantú, J. A. Galicia-Aguilar, D. Santamaria-Juárez and L. E. Hernández-Moreno, *Appl. Clay Sci.*, **121**, 146 (2016).
11. A. Guzmán, J. L. Nava, O. Coreño, I. Rodríguez and S. Gutiérrez, *Chemosphere*, **144**, 2113 (2016).
12. B. Ramavandi, G. Asgari, J. Faradmal, S. Sahebi and B. Roshani,

- Korean J. Chem. Eng.*, **31**, 2207 (2014).
13. A. H. Mahvi, M. Shalbafan, R. Nabizadeh, S. Nasser, S. Jorfi, B. Ramavandi and M. Ahmadi, *Toxin Reviews*, **36**, 52 (2017).
 14. R. Foroutan, M. Madani, M. R. Farani, A. K. Kori, E. Behrad and B. Ramavandi, *Int. J. Pharm. Technol.*, **8**, 25133 (2016).
 15. M. Ahmadi, E. Kouhgardi and B. Ramavandi, *Korean J. Chem. Eng.*, **33**, 2589 (2016).
 16. M. Fooladvand and B. Ramavandi, *Ind. J. Chem. Technol.*, **22**, 183 (2015).
 17. G. Asgari, B. Ramavandi and S. Sahebi, *Desal. Water Treat.*, **52**, 7354 (2014).
 18. G. Asgari, B. Ramavandi, L. Rasuli and M. Ahmadi, *Desal. Water Treat.*, **51**, 6009 (2013).
 19. W. Peng, H. Li, Y. Liu and S. Song, *J. Mol. Liq.*, **230**, 496 (2017).
 20. R. Foroutan, H. Esmaili, S. D. Rishehri, F. Sadeghzadeh, S. Mirahmadi, M. Kosarifard and B. Ramavandi, *Data in Brief*, **12**, 485 (2017).
 21. S. Delshab, E. Kouhgardi and B. Ramavandi, *Data in Brief*, **8**, 235 (2016).
 22. V. Alipour, S. Nasser, R. Nabizadeh Nodehi, A. H. Mahvi and A. Rashidi, *J. Environ. Health Sci. Eng.*, **12**, 146 (2014).
 23. H. Y. Yen and J. Y. Li, *J. Environ. Manage.*, **161**, 344 (2015).
 24. R. Foroutan, F. S. Khoo, B. Ramavandi and S. Abbasi, *Desal. Water Treat.*, **82**, 146 (2017).
 25. W. E. Federation and A. P. H. Association, *Standard methods for the examination of water and wastewater*, American Public Health Association (APHA): Washington, DC, U.S.A. (2005).
 26. D. Alidoust, M. Kawahigashi, S. Yoshizawa, H. Sumida and M. Watanabe, *J. Environ. Manage.*, **150**, 103 (2015).
 27. B. Xiang, W. Fan, X. Yi, Z. Wang, F. Gao, Y. Li and H. Gu, *Carbohydr. Polym.*, **136**, 30 (2016).
 28. E. Khoramzadeh, B. Nasernejad and R. Halladj, *J. Taiwan Ins. Chem. Eng.*, **44**, 266 (2013).
 29. M. Zabihi, A. Haghighi Asl and A. Ahmadpour, *J. Hazard. Mater.*, **174**, 251 (2010).
 30. K. D. Brahman, T. G. Kazi, J. A. Baig, H. I. Afridi, S. S. Arain, S. Saraj, M. B. Arain and S. A. Arain, *Chemosphere*, **150**, 320 (2016).
 31. L. Hao, T. Zheng, J. Jiang, G. Zhang and P. Wang, *Chem. Eng. J.*, **292**, 163 (2016).
 32. M. S. Podder and C. B. Majumder, *J. Mol. Liq.*, **212**, 382 (2015).
 33. M. S. Podder and C. B. Majumder, *BioChem. Eng. J.*, **105**, 114 (2016).
 34. M. Ahmadi, H. Rahmani, B. Ramavandi and B. Kakavandi, *Desal. Water Treat.*, **76**, 265 (2017).
 35. M. Ahmadi, M. Foladivanda, N. Jaafarzadeh, Z. Ramezani, B. Ramavandi, S. Jorfi and B. Kakavandi, *J. Water Supply Res. T.*, **66**, 116 (2017).
 36. M. Shams, I. Nabipour, S. Dobaradaran, B. Ramavandi, M. Qasemi and M. Afsharnia, *Fresen. Environ. Bull.*, **22**, 722 (2013).
 37. M. Attari, S. S. Bukhari, H. Kazemian and S. Rohani, *J. Environ. Chem. Eng.*, **5**, 391 (2017).
 38. G. Jin, Y. Eom and T. G. Lee, *J. Ind. Eng. Chem.*, **42**, 46 (2016).
 39. T. A. Saleh, A. Sari and M. Tuzen, *J. Environ. Chem. Eng.*, **5**, 1079 (2017).
 40. Y. Khambhaty, K. Mody, S. Basha and B. Jha, *Sep. Sci. Technol.*, **43**, 1221 (2008).
 41. G. Bayramoğlu, I. Tuzun, G. Celik, M. Yilmaz and M. Y. Arica, *Int. J. Min. Process*, **81**, 35 (2006).
 42. M. Karmacharya, V. K. Gupta, I. Tyagi, S. Agarwal and V. Jha, *J. Mol. Liq.*, **216**, 836 (2016).
 43. O.-H. Kwon, J.-O. Kim, D.-W. Cho, R. Kumar, S. H. Baek, M. B. Kurade and B.-H. Jeon, *Chemosphere*, **160**, 126 (2016).
 44. A. Nashine and A. Tembhurkar, *J. Environ. Chem. Eng.*, **4**, 3267 (2016).
 45. S. Zavareh, M. Zarei, F. Darvishi and H. Azizi, *Chem. Eng. J.*, **273**, 610 (2015).
 46. M. A. Khan, M. Ngabura, T. S. Y. Choong, H. Masood and L. A. Chuah, *Biores. Technol.*, **103**, 35 (2012).
 47. C. Xiong, Q. Jia, X. Chen, G. Wang and C. Yao, *Ind. Eng. Chem. Res.*, **52**, 4978 (2013).
 48. S. B. Mortazavi, B. Ramavandi and G. Moussavi, *Environ. Technol.*, **32**, 251 (2011).
 49. N. Habibi, P. Rouhi and B. Ramavandi, *Data in Brief*, **13**, 749 (2017).
 50. F. Deniz and A. Karabulut, *Ecol. Eng.*, **106**, 101 (2017).
 51. Q. Zheng, Z. Li, X. Miao, J. Li, Y. Huang, H. Xia and C. Xiong, *Appl. Organomet. Chem.*, **31**, 3546 (2017).